Observations of Radio Sources at 10.03 MHz*

A. H. Bridle
Astronomy Group, Department of Physics, Queen's University, Kingston, Canada

AND

C. R. Purton†
Radio Astronomy Section, Radio and Electrical Engineering Division, National Research Council, Ottawa, Canada

(Received 15 July 1968)

Flux densities are derived for 124 radio sources which have been observed with the 10.03 MHz telescope at the Dominion Radio Astrophysical Observatory. The procedure used to correct the observations for ionospheric effects, and the method of calibration of the flux density scale are described.

INTRODUCTION

STUDIES of discrete radio sources at frequencies less than 20 MHz are severely hindered by ionospheric absorption and scintillation, and for this reason very few sources had been observed at such frequencies until the recent period of minimal solar activity. Typical values of the total electron content of the ionosphere were particularly low during this period, and observations could therefore be made at frequencies that are unsuitable for radio astronomy during most of the solar cycle. This paper presents the results of observations of discrete sources made between October 1965 and March 1966 with the 10.03 MHz telescope at the Dominion Radio Astrophysical Observatory, Penticton, Canada.

EQUIPMENT

The antenna and receivers have been described fully by Galt, Purton, and Scheuer (1967), and are not discussed in detail here. The antenna is a T-shaped array of 400 dipoles; the arms of the T are of length 1242 m (41.4λ) east–west and 720 m (24λ) north–south. The two arms are used as an interferometer of zero spacing in the manner of a Mills cross (Mills, Little, Sheridan, and Slee 1958) to provide a reception pattern 2°.6 in right ascension by 2°.3 sec (zenith angle) in declination, between half-power points. Simultaneous observations can be made with a number of reception patterns directed to different declinations, to increase the rate at which data are obtained during periods free of ionospheric disturbances and terrestrial interference.

The observations described here were made with 180° switching receivers using a bandwidth of 8 kHz and an integration time of 90 sec. The predominant component of the noise on the output records was that produced by the background radiation. The peak noise deflection on an individual record was equivalent to that produced by a discrete source with a flux density of 60 flux units (1 f.u.$=10^{-26}$ W m^{-2} Hz^{-1}) when the reception pattern was directed away from the galactic equator. For most observations this noise level was reduced to an equivalent flux density of 20 f.u. by repeating the observations and by averaging of the individual records during their reduction. The accuracy of the observations was limited by source confusion, one source being expected in every 20 areas of the reception pattern at a flux density of $\approx$100 f.u.

METHOD OF OBSERVATION

Sources were observed at meridian transit. The method of phasing the antenna response in declination (Galt, Purton, and Scheuer 1967) produced 64 reception patterns at fixed declinations and a source was normally observed in the pattern that provided the maximum antenna gain at its declination. Three receivers were available, and the remaining reception patterns could be used either to make simultaneous observations of the same source with adjacent reception patterns, and thus to measure its apparent declination, or to observe other sources at similar right ascensions. The latter procedure was adopted for sources that were insufficiently intense to be observable in more than one of the available reception patterns.

A typical observation is shown in Fig. 1, which was obtained at a transit of 3C274 (Vir A). The level of the background radiation was recorded before and after the transit of a source so that the profile of the radiation against which the source is observed could be

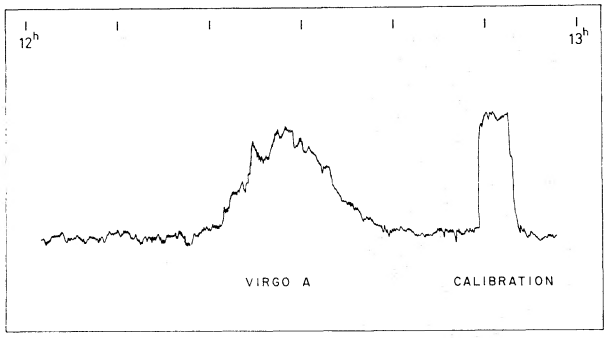

FIG. 1. Record of the radio source 3C274 obtained with this instrument. The fluctuations of the record near the peak deflection are caused by ionospheric scintillations.

* Dominion Observatory Contrib. No. 251.

† Present address: Centre for Research in Experimental Space Science, York University, Toronto, Canada.

derived. Each observation was followed by a calibration of the sensitivity of the receiver made by injecting noise power coherently into each arm of the antenna and noting the deflection of the output record.

The positions of the sources observed were determined only with the accuracy required to identify them in the Third Cambridge Catalogue (Edge, Shakeshaft, McAdam, Baldwin, and Archer 1959) or, in some cases, in the Fourth Cambridge Catalogue (Pilkington and Scott 1965; Gower, Scott, and Wills 1967). An accuracy of $\pm 0^\circ.5$ in each coordinate was normally sufficient for this purpose.

IONOSPHERIC EFFECTS

The effects of the ionosphere on observations at 10 MHz could be severe, even though the work was carried out at the most favorable phase of the solar cycle. The principal ionospheric effects are absorption, refraction, and scintillation.

The ionospheric absorption at the time of an observation was estimated from continuous records of the background radiation at the zenith made using the north–south arm of the antenna with a total-power radiometer. The variation of the observed background brightness at each hour of right ascension throughout the period 1965 July to 1966 July was derived from these records. The absorption at a given time during this period was estimated by comparing the brightness observed at this time with the maximum brightness observed during the year at the same right ascension.

This method of estimating absorption assumes that the brightness that would be observed at a given point in the sky in the absence of absorption is correctly estimated by the maximum brightness observed, i.e., that every part of the sky was observed under conditions of vanishingly small absorption at some time during the year. The following considerations suggest that this assumption is valid. The critical frequency of the F_2 layer, f_0F_2, measured by ionosonde equipment at Kenora, Ontario, and Ottawa, Ontario (Canadian Ionospheric Data, Department of Transport, 1965–1966), which are at similar geomagnetic latitudes to Perticton, was frequently <2 MHz on winter nights throughout the observing period. Ellis (1963) has shown that the absorption by the F_2 layer at these times would be <0.05 dB at 10 MHz. Provided there is no component of the nighttime absorption which is uncorrelated with F_2 layer parameters, the hours of right ascension which transit on the meridian during winter nighttime will therefore be observed in almost absorption-free conditions on some occasions. Furthermore, for these hours of right ascension the maximum value of the brightness was observed on a large number of nights, and no relative absorption could be detected at times when f_0F_2 was <2 MHz. This independently suggests that on these occasions the absolute absorption was close to zero. The brightnesses for right ascensions between 17^h and 21^h did not exhibit such well-defined maxima, and it is likely that these hours, which transit the meridian during summer nighttime, were rarely observed in the absence of absorption. The "unabsorbed" brightnesses for these hours were therefore estimated from an analysis of the equinoctial absorption data. The curves showing the variation of the mean absorption with local time for the two equinoxes should be similar in form (Roger 1968); the absorption between 17^h and 21^h right ascension was scaled to that between 3^h and 7^h right ascension with this assumption. The daily absorption curves were averaged over the seven days closest to the two equinoxes to obtain the mean curves for this analysis.

The absorption derived from the total-power records in this way is that occurring near the zenith. Observations of sources away from the zenith were corrected for absorption assuming that the absorbing layer is a spherical shell in which the electron density–radius profile does not vary with latitude. Daytime values of the absorption could be as high as 5 dB due to absorption by the D layer, and all radio source observations were made at night to avoid the need for such large corrections. During winter nights the absorption at the zenith was rarely greater than 0.5 dB, and the subsidiary correction for zenith angle dependence of the absorption was rarely greater than 0.2 dB. The majority of transits have been reduced with an absorption correction which is thought to be within ± 0.2 dB of the "true" absorption.

Ionospheric refraction in the east–west plane altered only the time of transit of a source and presented few problems. Because fixed declination settings of the reception pattern were employed, refraction in the north–south plane affected the antenna gain in the direction of a source and this effect had to be taken into account in reducing the records. The predominant effect in the north–south plane was wedge refraction arising from a southward enhancement of electron density, so that the apparent positions of all radio sources were displaced toward the south. The magnitude of the displacement at a particular time could be found by observing intense sources with adjacent reception patterns as described above. Transits of some sources which were too weak to be observed in more than one reception pattern were reduced using refraction data obtained from transits of intense sources throughout the same night. It was not, however, possible to determine the north–south refraction for $\approx 50\%$ of transits of weak sources because the appropriate records of intense sources could not be obtained due to the onset of interference or severe scintillation. Corrections derived from averaging the observed refraction of 20 intense sources over a period of several months were applied to these transits. The typical variation of the north–south refraction near the zenith from night to night, and throughout any one

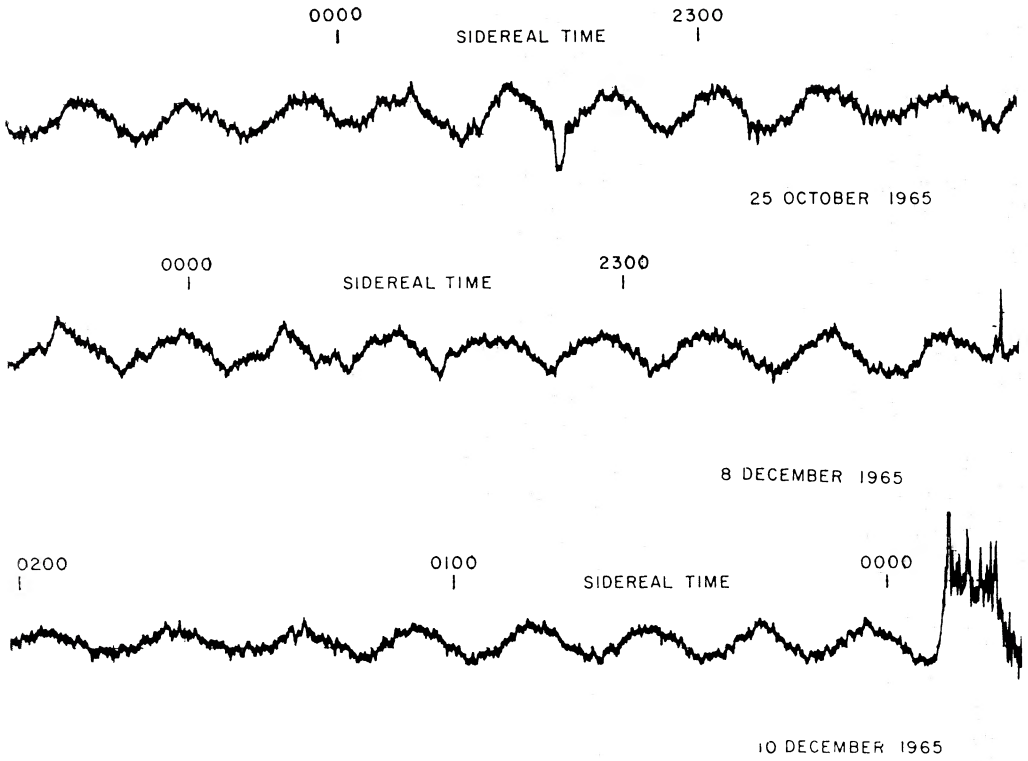

FIG. 2. Records of the radio source Cas A obtained with a 10.05 MHz interferometer at 30 wavelengths spacing (Bridle 1967).

night, was $\approx 0^{\circ}.25$ about a mean value of $0^{\circ}.5$, so that the application of a mean correction is not entirely satisfactory. The flux densities derived from transits that were reduced using the mean refraction correction are less mutually consistent than those derived from transits reduced using measured refraction. The errors arising from this effect are included in the final error estimates for individual sources.

Severe ionospheric scintillation could make the voltages induced in the two arms of the antenna incoherent, so that the theoretical reception pattern was not achieved. In extreme conditions the output consisted of a series of "spikes" of irregular amplitude and duration near the expected times of transit of intense sources; on such occasions sources whose flux densities were close to the normal instrumental limit could not be distinguished on the records at all. Scintillation conditions were monitored throughout each observing period by recording transits of intense sources using a time constant of 10 sec, and records obtained at times when scintillations introduced fluctuations $>50\%$ of source intensities were discarded. Scintillations were most severe at night, so conditions of low absorption and little scintillation were rarely realized together. Between October 1965 and March 1966 ≈ 30 nights were substantially free of both effects, and most of the results presented here were obtained on these nights.

TERRESTRIAL INTERFERENCE

The operating frequency of 10.03 MHz was selected after a period of trial observations at a number of frequencies between 10.00 and 10.05 MHz. The 8 kHz bandwidth centered on this frequency was largely free of interference at night, but observations were only occasionally possible during daylight. The effective restriction to nighttime observing imposed by interference and absorption has prevented us from observing more than a very few sources between right ascensions 17^{h} and 21^{h}. At other right ascensions the coverage of the sky was limited mainly by the incidence of scintillation, and by the variation of the antenna gain with zenith angle, which is discussed below.

CALIBRATION OF THE OBSERVATIONS

The sensitivity of the receiver was calibrated using temperature-limited noise diodes whose relative outputs were compared by connecting them to the receiver through standard attenuators. As discussed below, the flux density scale was derived by observing the source Cas A, whose flux density at 10 MHz was measured in an independent experiment (Bridle 1967). For these observations, the calibration noise was applied in several increments to investigate the linearity of the receiver at high flux densities; the correction for non-

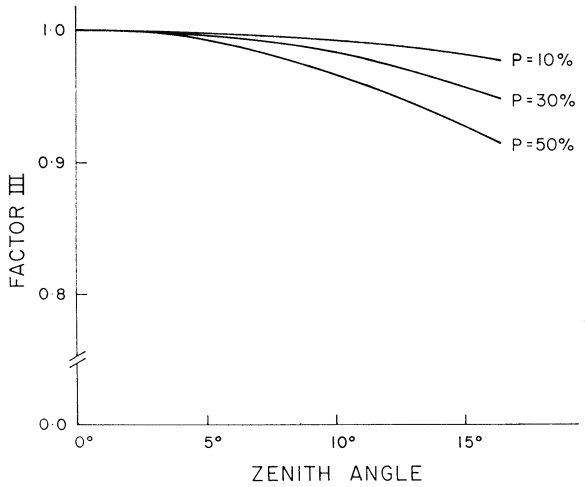

FIG. 3. Factor (3) of the $G(z)$ curve at $z<15°$ for different assumed values of P.

linearity was found to be insignificant compared with the uncertainties in the ionospheric corrections.

The absolute calibration of the antenna gain presented a more difficult problem. At higher frequencies the gains of complex antennas are usually determined by observing sources whose flux densities have been measured using smaller antennas for which the gains can be computed reliably. At low frequencies such calibration measurements are restricted to small arrays of dipoles. Only Cas A and Cyg A have sufficiently high flux densities to be measured accurately with such antennas, and Cyg A is unfortunately situated in the area of sky that transits during the nighttime in the summer, so that low-frequency measurements of this source are severely hindered by ionospheric effects. Cas A is not ideal as a calibration source because of the curvature of its low-frequency radio spectrum and its secular variation of intensity. The spectral curvature of this source is defined by three independent measurements, at 3.0 MHz (Parthasarathy 1967), 10.05 MHz (Bridle 1967), and 13.1 MHz (Purton 1966). The flux density observed at 3.0 MHz is too high to be consistent with the measurements at 10.05 MHz and 13.1 MHz, assuming a simple spectral law for the source. The published 3.0 MHz records appear seriously affected by scintillation, which could easily lead to an overestimate of the flux density. The 10.05 MHz and 13.1 MHz records were not so seriously affected by scintillation, as may be expected from the higher observing frequencies and the greater distances of these experiments from the auroral zone. Examples of records from the 10.05 MHz experiment are given in Fig. 2. This experiment was carried out at the mean epoch of our observations, and at very nearly the same frequency, so the use of its result to calibrate our observations eliminates uncertainty that might arise either from the spectral curvature or from the secular decrease in intensity. This measurement has therefore been adopted as a calibration standard.

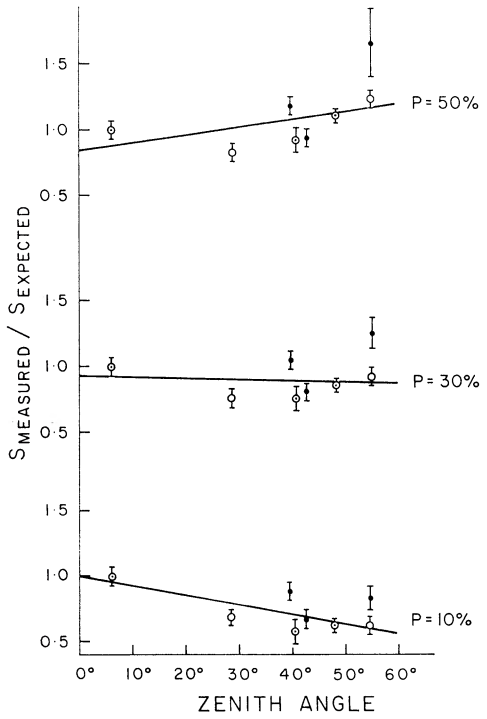

FIG. 4. The ratio of observed to extrapolated flux densities of radio sources identified with elliptical galaxies plotted against zenith angle for several assumed values of P. The data was weighted according to the quality of the records (3:2:1 for points shown as ⊙, ○, and ●, respectively) to derive the best-fit lines shown here.

The relative gain within any of the 64 available reception patterns may easily be computed, but since only one calibration source is available at 10 MHz, the absolute gain is only known for one reception pattern. An important further problem has therefore been to find the relation between the values of the maximum gains of the reception patterns at different zenith angles. We refer to this as the gain–zenith angle $G(z)$ relation.

The form of $G(z)$ for this antenna depends on:

(1) The variation with z of the directivity D (Pawsey and Bracewell 1955).

(2) The variation with z of the power reflected from the antenna.

(3) The proportion of the total power received in randomly distributed "error" sidelobes that result from random residual errors in phase, attenuation, and impedance within the feeder system. We call this proportion P.

The effects of factors (1) and (2) can be evaluated precisely from a knowledge of the properties of the antenna and feeder system. The effects of interactions between antenna elements are particularly important and have been taken into account using experimentally determined mutual impedances for the array. The

effect of (3) depends critically on the magnitude of the errors in the feeder system, and this could not be measured with sufficient accuracy for our purpose. The effect was therefore computed for a range of assumed values of P, giving the family of curves shown in Fig. 3. This figure shows that the antenna gain is insensitive to factor (3) for zenith angles $z<15°$. The observations of Cas A could therefore be used together with the computed $G(z)$ at $z<15°$ to estimate the flux densities of sources near the zenith without incurring appreciable error from the uncertainty in P.

The observations of sources within 15° of the zenith showed that the flux densities of many sources at 10 MHz do not differ significantly from those expected by extrapolation of higher-frequency data to 10 MHz. In particular, the mean ratio of observed to extrapolated flux densities for six sources identified with elliptical galaxies at galactic latitudes $|b^{II}|>15°$ is 0.98 ± 0.15.

The 10 MHz flux densities of seven sources at $z>15°$ which are optically identified with elliptical galaxies at $|b^{II}|>15°$ were estimated by extrapolation of their radio spectra as determined by pencil-beam observations at 38 MHz (Williams, Kenderdine, and Baldwin 1966), at 178 MHz (Caswell 1966), and at 750 and 1400 MHz (Pauliny-Toth, Wade, and Heeschen 1966). The extrapolation did not include the 26.3 MHz data of Erickson and Cronyn (1965) since these authors obtained their calibration by a similar procedure. The sources, which are identified in Table I by †, were observed at 10 MHz in favorable conditions and have well-determined radio spectra at the higher frequencies. The extrapolation to 10 MHz could be in error if any of the spectra exhibited low-frequency cutoffs between 38 and 10 MHz. It is unlikely that the spectra of these sources would be affected by free–free absorption in interstellar ionized hydrogen in the Galaxy, because of the restriction to $|b^{II}|>15°$: only one of the sources is at $|b^{II}|<25°$. It is also unlikely that any of these sources would be affected by synchrotron self-absorption, since none has a brightness temperature at 178 MHz $>10^7$ °K.

The extrapolated 10 MHz flux densities of these sources were used to select the appropriate member of the family of curves shown in Fig. 3 by the following procedure. For several assumed values of P, the observations were used to derive 10 MHz flux densities for these sources. These flux densities were then compared with the extrapolated values, and P selected to achieve the best agreement. The flux densities obtained by these two methods are compared in Fig. 4 for various assumed values of P. The best agreement, indicated by a horizontal straight line in Fig. 4, was obtained for $P=(30\pm10)\%$. P will take this value if the rms deviation of the currents excited in the array from those which would exist if the feeder were ideal is $\pm6\%$ (Bracewell 1961).

The form of $G(z)$ derived from this analysis and adopted for the reduction of all observations is shown in Fig. 5. It may be noticed that the curve shown is not smooth; this is because the east–west arm of the antenna was phased in zenith angle in coarser steps than the north–south arm. It may also be noticed that G varies relatively slowly with z for $z<30°$. This arises from the way in which the antenna was coupled to the feeder system, which led to optimum matching for $z\approx30°$. In this circumstance the effects of factors (1) and (2) are in opposition as z increases from 0° to 30° (Fig. 6). A full account of the analysis of the performance of the antenna will be presented elsewhere (Purton, to be published).

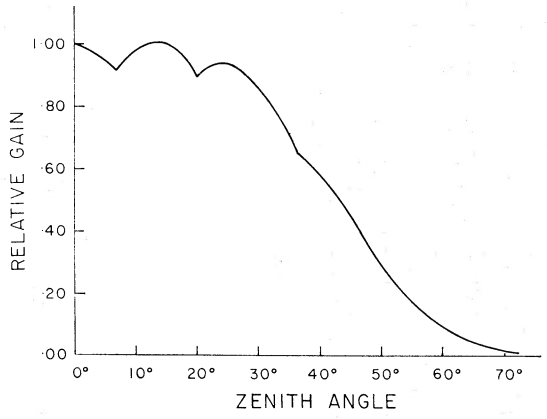

FIG. 5. The derived $G(z)$ relation for the 10.03 MHz telescope.

ANALYSIS OF RECORDS

Source transits were analyzed by fitting the theoretical right ascension response pattern to the records obtained, after subtracting the estimated background profile. Uncertainties in determining this profile were small compared with uncertainties in the ionospheric corrections for most sources, but became significant for sources close to intense galactic structure. The effects of these uncertainties are included in the quoted errors in individual flux densities. The total energy received by the antenna during a transit is unaltered

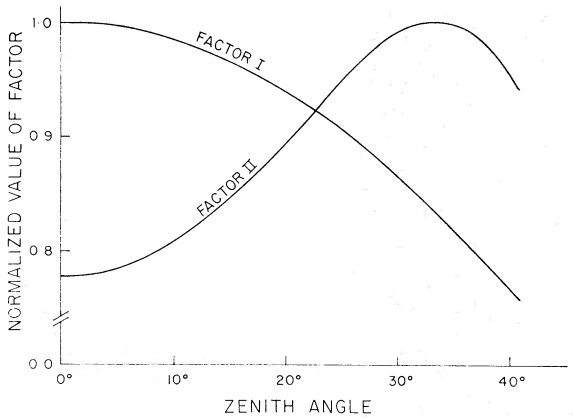

FIG. 6. Factors (1) and (2) of the $G(z)$ curve at $z<40°$.

TABLE I.

Serial number	Source	10.03 MHz flux density (f.u.)	Notes
DB 1	3C9	170± 35	constant spectral index below ≈100 MHz
DB 2	3C10	350± 110	maximum flux density between 10 and 22 MHz
DB 3	*3C20	205± 60	corrected for confusion by 3C22; spectral index may decrease below 25 MHz
DB 4	3C22	140± 25	corrected for confusion by 3C20; uncertain spectrum
DB 5	3C27	160± 40	constant spectral index
DB 6	3C31	120± 40	corrected for confusion by 3C34; constant spectral index
DB 7	†3C33	490± 100	possibly complex spectrum
DB 8	*3C34	200± 60	corrected for confusion by 3C31; constant spectral index
DB 9	*3C35	155± 30	spectral index may decrease below 100 MHz
DB 10	*3C47	260± 60	spectral index decreases below 22 MHz
DB 11	0135+30°.1	110± 40	±1° uncertainty in declination
DB 12	*3C55	150± 60	spectral index decreases with decreasing frequency
DB 13	*3C66	560± 100	corrected for confusion by 4C42.6; spectral index increases with decreasing frequency below 38 MHz
DB 14	*3C65	150± 30	constant spectral index
DB 15	3C68.1	130± 25	spectral index decreases with decreasing frequency
DB 16	*3C68.2	185± 50	spectral index decreases with decreasing frequency
DB 17	*4C28.6	170± 50	constant spectral index
DB 18	4C39.10	105± 25	confused with 4C39.9 and 4C38.8
DB 19	3C75	380± 120	spectral index may increase with decreasing frequency
DB 20	*4C35.6	155± 40	possibly resolved at 178 MHz
DB 21	3C79	210± 55	constant spectral index
DB 22	*3C84	1420± 320	corrected for confusion with 3C83.1; spectral index increases with decreasing frequency
DB 23	*3C86	185± 50	constant spectral index
DB 24	†3C89	560± 170	constant spectral index
DB 25	†3C98	210± 55	spectral index decreases below 20 MHz
DB 26	4C14.9 4C14.10	190± 45	combined spectrum may have constant spectral index
DB 27	*3C103	160± 40	spectral index may decrease below 22 MHz
DB 28	3C109	175± 45	constant spectral index
DB 29	0416+13°.9	240± 80	±0°.9 uncertainty in declination
DB 30	*3C111	360± 80	spectral index decreases below 22 MHz
DB 31	*3C123	800± 160	spectral index decreases below 22 MHz
DB 32	*3C129	270± 55	includes 3C129.1; constant spectral index
DB 33	3C130	110± 30	constant spectral index
DB 34	*3C131	470± 200	corrected for confusion by 4C33.10; spectral index increases with decreasing frequency below 38 MHz
DB 35	*HB9	800± 200	diameter 1°.9±0°.4 in both coordinates at 10 MHz; integrated flux density given
DB 36	3C133	100± 30	constant spectral index
DB 37	*3C134	520± 90	spectral index decreases below 25 MHz
DB 38	*3C144	4650±1200	constant spectral index, but may be affected by interstellar H II absorption
DB 39	*3C153 4C47.19	245± 45	spectral index of combined spectrum increases with decreasing frequency
DB 40	3C154	95± 30	spectral index decreases below 25 MHz
DB 41	*3C157	400± 100	spectral index decreases below 25 MHz
DB 42	3C158	200± 50	constant spectral index below 100 MHz
DB 43	3C166	125± 30	spectral index may decrease below 30 MHz
DB 44	3C172	130± 40	constant spectral index
DB 45	3C175	175± 65	spectral index may decrease below 40 MHz
DB 46	4C12.29 4C12.30	330± 150	combined spectrum may have constant spectral index
DB 47	*4C24.15	230± 45	spectrum uncertain
DB 48	*4C21.23	185± 65	constant spectral index
DB 49	3C186	95± 30	spectral index decreases with decreasing frequency
DB 50	*4C56.16	160± 35	spectrum uncertain
DB 51	3C190	160± 35	constant spectral index
DB 52	3C191	230± 55	constant spectral index
DB 53	*†3C192	155± 40	constant spectral index
DB 54	*3C196	340± 70	spectral index decreases with decreasing frequency
DB 55	3C198	220± 80	possibly complex spectrum
DB 56	3C199	125± 35	4C43.16 and 4C44.17; constant spectral index
DB 57	3C200	140± 35	constant spectral index
DB 58	4C11.28	190± 50	constant spectral index
DB 59	3C205	135± 30	constant spectral index
DB 60	*4C29.31	210± 60	spectral index may increase with decreasing frequency
DB 61	0855+10°.5	330± 90	±1° uncertainty in declination
DB 62	3C215	140± 40	constant spectral index
DB 63	4C18.28	120± 60	corrected for confusion by 4C18.27; spectral index may increase with decreasing frequency below 50 MHz

TABLE I (*continued*)

Serial number	Source	10.03 MHz flux density (f.u.)	Notes
DB 64	*4C38.27	260± 100	corrected for confusion with 3C217; constant spectral index
DB 65	3C218	9100±3500	very large ionospheric corrections at 10 MHz; probably constant spectral index
DB 66	*3C219	330± 75	constant spectral index
DB 67	4C31.33	105± 25	spectrum uncertain
DB 68	4C14.31	175± 40	constant spectral index
DB 69	3C225	125± 45	spectral index decreases with decreasing frequency
DB 70	3C227	560± 130	spectral index may increase with decreasing frequency
DB 71	3C228	165± 35	constant spectral index
DB 72	*3C234	340± 80	constant spectral index
DB 73	{3C237 3C238}	185± 45	combined spectrum has constant spectral index
DB 74	{4C39.29 4C39.30}	125± 30	spectrum uncertain
DB 75	*3C244.1	180± 35	constant spectral index
DB 76	3C245	150± 35	constant spectral index
DB 77	1054+18°.6	235± 60	±1°.1 uncertainty in declination
DB 78	*3C250	300± 70	constant spectral index
DB 79	3C252	120± 40	spectral index decreases below 38 MHz
DB 80	*3C254	160± 30	may be affected by Cas A sidelobe; spectral index probably decreases with decreasing frequency
DB 81	3C263.1	120± 30	constant spectral index
DB 82	3C264	630± 125	spectral index increases with decreasing frequency
DB 83	*4C55.22	230± 80	constant spectral index
DB 84	3C268.1	185± 50	constant spectral index
DB 85	†3C274	8300±2000	constant spectral index
DB 86	1249+57°.9	100± 30	±1° uncertainty in declination; possibly includes 3C277.1
DB 87	*3C280	160± 30	constant spectral index
DB 88	*Coma Cluster	360± 70	corrected for confusion by 3C277.3; spectral index increases with decreasing frequency
DB 89	*1305+46°.7	150± 30	spectrum uncertain; 38 MHz declination
DB 90	3C284	105± 25	confused by DB 88; spectral index may decrease with decreasing frequency
DB 91	*3C288	165± 40	constant spectral index
DB 92	*3C293	155± 30	spectral index may increase with decreasing frequency below 100 MHz
DB 93	4C31.44	100± 35	spectrum uncertain
DB 94	3C300	240± 50	constant spectral index
DB 95	4C48.38	120± 45	constant spectral index
DB 96	*4C38.39	180± 45	spectrum uncertain
DB 97	*4C47.39	150± 50	constant spectral index
DB 98	*3C310	500± 140	spectral index decreases with decreasing frequency
DB 99	*3C315	165± 55	confused by 3C310; constant spectral index
DB 100	*1522+43°.6	150± 30	±0°.9 uncertainty in declination
DB 101	3C319	125± 30	constant spectral index below 178 MHz
DB 102	*3C321	170± 45	constant spectral index
DB 103	3C322	110± 20	constant spectral index
DB 104	{3C327 3C327.1}	1000± 300	combined spectrum has constant spectral index
DB 105	4C44.27	130± 40	constant spectral index
DB 106	*3C330	150± 50	constant spectral index
DB 107	*4C35.40	160± 60	spectrum uncertain
DB 108	*3C336	160± 50	constant spectral index
DB 109	*3C337	160± 50	corrected for confusion with 4C43.38; spectral index increases with decreasing frequency
DB 110	*3C338	340± 65	spectral index decreases with decreasing frequency
DB 111	†3C348	5000±1000	constant spectral index
DB 112	†3C353	2000± 500	constant spectral index
DB 113	3C356	110± 25	spectral index decreases with decreasing frequency
DB 114	4C48.45	140± 25	constant spectral index
DB 115	3C380	140± 25	maximum flux density between 10 and 22 MHz
DB 116	3C388	260± 70	constant spectral index
DB 117	3C405	13500±3500	Cyg A; flux density from Bridle 1967
DB 118	3C409	430± 130	maximum flux density between 10 and 22 MHz
DB 119	Cygnus Loop	1300± 350	NGC 6960, NGC 6992-5; diameter 2°.2±0°.5 NS at 10 MHz; integrated flux density given
DB 120	3C430	190± 45	maximum flux density between 10 and 22 MHz
DB 121	3C438	120± 30	maximum flux density between 10 and 22 MHz
BD 122	3C452	330± 90	spectral index decreases below 22 MHz
DB 123	3C461	28000±2800	Cas A; flux density from Bridle 1967
DB 124	3C465	400± 70	constant spectral index

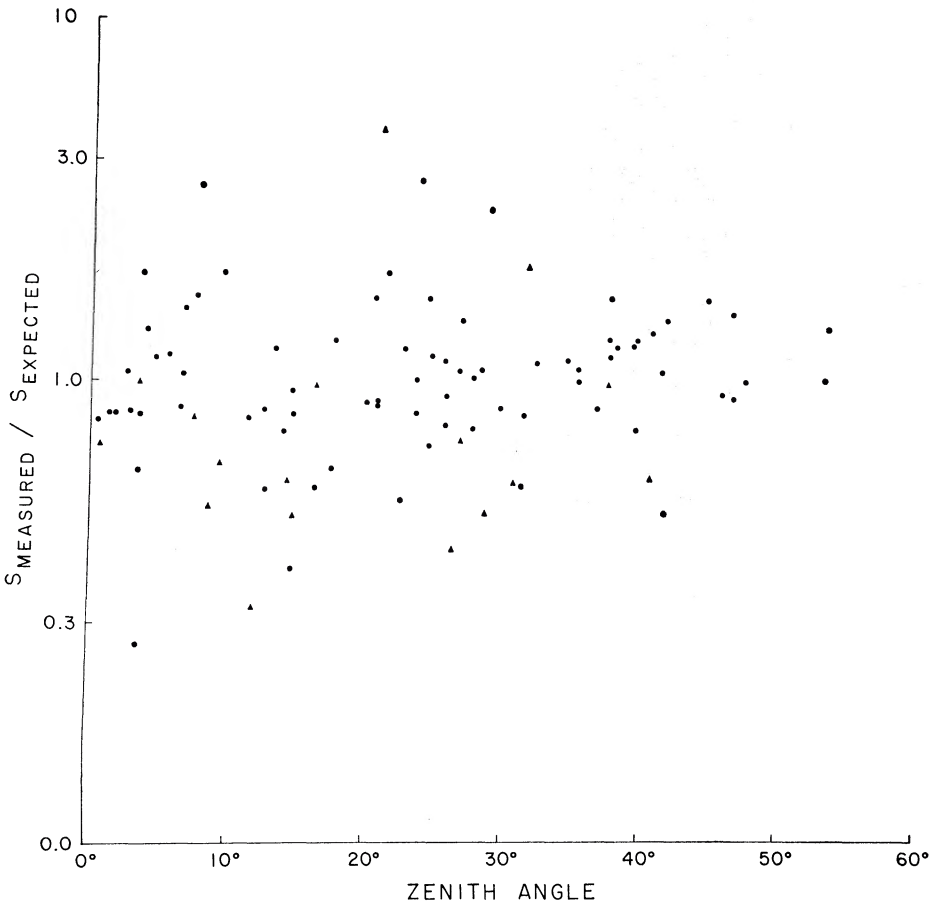

FIG. 7. The ratio of observed to extrapolated flux densities for the sources observed, plotted against the zenith angle of the observations ($\blacktriangle b^{II} \leqslant 10°$, $\bullet b^{II} > 10°$).

by scintillation if the voltages induced in the two arms remain correlated. Records should therefore deviate above and below the theoretical response in such a way that the area enclosed between them is algebraically zero, and this criterion was adopted to obtain the best fit.

The deflection of the output record at the maximum of the fitted response was corrected for ionospheric absorption and for variation in the receiver sensitivity. The theoretical value of the antenna gain, allowing for refraction, was then used to obtain the calibration noise power to which the source would be equivalent if observed at the zenith and in the absence of the ionosphere. The flux density of the source was then derived by comparing this noise power with the corresponding value obtained from the observations of Cas A.

OBSERVATIONS

The first series of observations included sources from the Revised Third Cambridge Catalogue (Bennett 1962) whose flux densities at 10 MHz were expected to exceed 200 f.u./(1 f.u.$=10^{-26}$Wm^{-2}Hz^{-1}) from the evidence of their higher-frequency spectra. A number of extended sources not included in this catalogue were also observed.

The observations were later extended to include some sources whose flux densities were expected to lie in the range 100 to 200 f.u. In this range the 10 MHz observations included some sources whose flux densities at 178 MHz are less than the limiting flux density of the Revised Third Cambridge Catalogue, but which are listed in the Fourth Cambridge Catalogue (Pilkington and Scott 1965; Gower, Scott, and Wills 1967). The spectral indices of sources in this catalogue were not known at the time of these observations, and so it was not possible to use this catalogue as a "finding list" at 10 MHz. Sources from this catalogue were observed if measurements at 26.3 MHz (Erickson and Cronyn 1965) or 22.25 MHz (Costain, personal communication) had previously indicated that their spectral indices were unusually high, or if they were detected unexpectedly while other sources were being observed at 10 MHz.

In order to investigate the statistics of radio spectra at this frequency, a homogeneous sample of sources was obtained by systematically surveying the area of sky between declinations $+20°$ and $+60°$, and right ascensions 0^h and 16^h30^m. Within this area all sources with flux densities at 10 MHz $\geqslant$ 150 f.u. should have been observed, with only a small number of random omissions due to interference or to confusion with

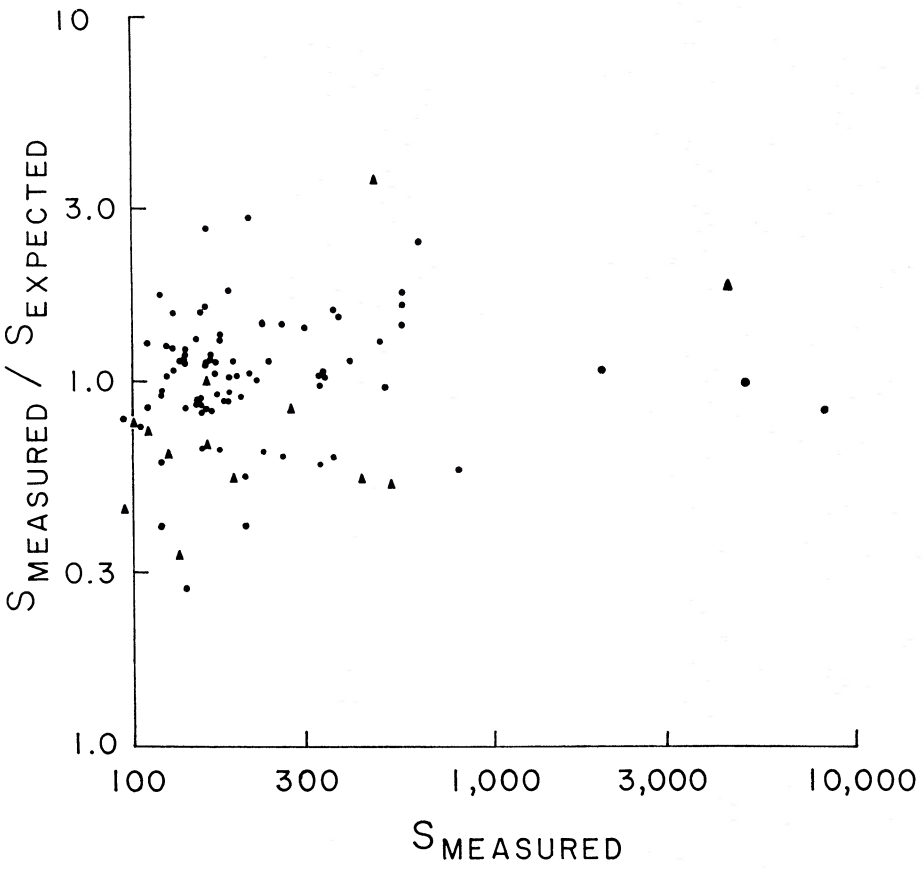

FIG. 8. The ratio of observed to extrapolated flux densities for the sources observed, plotted against the observed flux densities S($\blacktriangle b^{II} \leqslant 10°$, $\bullet b^{II} > 10°$).

sidelobe responses of the antenna. The principal areas within which the sample may be incomplete are (i) within 15° of the galactic equator; (ii) between declinations +20° and +35° at right ascensions 5^h to 6^h, due to disturbance of these records by intense Jupiter bursts; and (iii) between declinations +20° and +30° at right ascensions 12^h to 13^h, due to sidelobe responses to 3C274 (Vir A). The source 3C28 has not been included due to poor quality of the records, and the sources 3C324, 3C326, and 3C326.1 have not been included due to inadequate resolution by the antenna response.

The sources which form this sample are denoted in Table I by *. The sample is suitable for statistical analysis because no astronomically significant bias exists in its selection, and omissions from it should be random. The radio spectra of the sources it contains are discussed elsewhere (Williams and Bridle 1967; Bridle, Costain, and Roger, to be published).

The observational results are given in Tables I and II. Table I lists flux densities for 124 sources, and Table II lists upper limits to the flux densities of 8 sources that were not detected on several occasions when observations of sources in neighboring areas of sky showed that observing conditions were favorable. The sources in Table I are listed in order of increasing right ascension and are given serial numbers with the prefix DB [for "Dominion—list B"; list A is a survey of radio sources at 1420 MHz (Galt and Kennedy 1968)]. Sources are also given their numbers from the Cambridge catalogues where possible; several sources whose identifications in these catalogues are not clear are assigned numbers that specify their observed (1966.0) right ascension and declination in hours and minutes of right ascension followed by degrees of declination. The flux densities are given in flux units, with their rms errors. These errors include the effects of uncertain ionospheric corrections, of the uncertainties in the antenna gain at high zenith angles, and errors in the absolute measurement of the flux density

TABLE II.

Source	10.03 MHz flux density (f.u.)	Notes
3C19	< 90	
3C69	⩽200	
3C125	<200	
3C216	< 90	maximum flux density between 10 and 22 MHz
3C239	<100	spectral index decreases with decreasing frequency
3C265	<160	spectral index decreases with decreasing frequency
3C294	<170	
3C334	<130	

of Cas A, as well as estimates of the errors in reducing the records. The final column of the table gives supplementary notes to each source, and indicates briefly the form of the radio spectrum of the source, taking the new observations into account.

It should be emphasized that in areas of sky outside the "sample area" defined earlier, the results given in Table I are not complete to any particular flux density limit; at zenith angles $>32°$ only the most intense sources have been measured because at these zenith angles the antenna gain is reduced and also ionospheric difficulties are greater. The coverage of the hours of right ascension between 16^h30^m and 24^h is also incomplete due to ionospheric difficulties.

In Figs. 7 and 8 the ratios of observed to extrapolated flux densities at 10 MHz are plotted against the zenith angle and the observed flux density, respectively, for all sources observed in this work whose spectra are well determined at higher frequencies. Neither figure shows evidence of bias in the observations, and it is concluded that the data are free from systematic effects depending on either the zenith angle of an observation or on the flux density of the source observed.

The flux densities of approximately 200 sources were measured with the 22.25 MHz telescope (Costain, Roger, and Lacey 1968) at the Dominion Radio Astrophysical Observatory while this work was in progress, and the spectral data provided by these two sets of observations will be discussed in detail in a later paper (Bridle, Roger, and Costain, to be published).

ACKNOWLEDGMENTS

The telescope was a joint project of the Dominion Radio Astrophysical Observatory, Penticton, Canada, and the Mullard Radio Astronomy Observatory, Cambridge, England. The authors were the guests of the DRAO for the period of this work and gratefully acknowledge its kind hospitality. Dr. J. A. Galt, Mr. A. R. Hamilton, Mr. M. D. Robinson, and Mr. E. W. Orge made invaluable contributions to the regular operation of the telescope, and Dr. C. H. Costain, Dr. J. A. Galt, Dr. R. S. Roger, and Dr. P. A. G. Scheuer are thanked for helpful discussions.

The authors also wish to thank the National Research Council of Canada, the U.K. Science Research Council, and the Cavendish Laboratory, Cambridge, for financial assistance during the performance of this work.

REFERENCES

Bennett, A. S. 1962, *Mem. Roy. Astron. Soc.* **68**, 163.
Bracewell, R. N. 1961, *Trans. Antennas Prop.* **AP-9**, 49.
Bridle, A. H. 1967, *Observatory* **87**, 60.
Caswell, J. L. 1966, Ph.D. thesis, University of Cambridge.
Costain, C. H., Roger, R. S., and Lacey, J. D. 1968, *Trans. Antennas Prop.* (to be published).
Edge, D. O., Shakeshaft, J. R., McAdam, W. B., Baldwin, J. E., and Archer, S. 1959, *Mem. Roy. Astron. Soc.* **68**, 37.
Ellis, G. R. A. 1963, *Australian J. Phys.* **16**, 411.
Erickson, W. C., and Cronyn, W. M. 1965, *Astrophys. J.* **142**, 1156.
Galt, J. A., and Kennedy, J. E. D. 1968, *Astron. J.* **73**, 135.
Galt, J. A., Purton, C. R., and Scheuer, P. A. G. 1967, *Publ. Dominion Obs.* **XXV**, 10.
Gower, J. F. R., Scott, P. F., and Wills, D. 1967, *Mem. Roy. Astron. Soc.* **71**, 49.
Mills, B. Y., Little, A. G., Sheridan, K. V., and Slee, O. B. 1958, *Proc. Inst. Radio Engrs.* **46**, 67.
Parthasarathy, R. 1967, *Science* **158**, 1449.
Pauliny-Toth, I. I. K., Wade, C. M., and Heeschen, D. S. 1966, *Astrophys. J. Suppl.* **XIII**, 65.
Pawsey, J. L., and Bracewell, R. N. 1955, *Radio Astronomy* (Oxford University Press, New York).
Pilkington, J. D. H., and Scott, P. F. 1965, *Mem. Roy. Astron. Soc.* **69**, 183.
Purton, C. R. 1966, Ph. D. thesis, University of Cambridge.
Roger, R. S. 1968 (to be published).
Williams, P. J. S., Kenderdine, S., and Baldwin, J. E. 1966, *Mem. Roy. Astron. Soc.* **70**, 53.
Williams, P. J. S., and Bridle, A. H. 1967, *Observatory* **87**, 280.